Vertical Vibration Response of Footbridges with Fundamental Natural Frequency up to 10 Hz under Dynamic Loading by Single Pedestrian

M. García-Diéguez[1]; J. L. Zapico-Valle[2]; and S. Živanović[3]

Abstract: A design spectrum of characteristic acceleration response to pedestrian-induced dynamic loading has been developed for footbridge structures. The novelty of the proposed spectrum over the existing spectra is that: (1) it is underpinned by a recently developed comprehensive statistical model of pedestrian dynamic loading; (2) it is applicable to a broader natural frequency range of structures up to 10 Hz; and (3) it accounts for uncertainties in both dynamic loading and structure dynamics that are typically encountered in structural design. In addition, the importance of correct modeling of pedestrian's walking speed and narrow-band nature of the force signal has been demonstrated. Comparison with the design spectra recommended in contemporary design codes reveals that the existing approaches are not being applicable for structures with natural frequency in the range of third, fourth, and fifth harmonic of the dynamic force. In addition, they could both underestimate and overestimate the structural response for lower-frequency structures. The proposed design spectrum is a design tool applicable to structures whose mode shape can be approximated by half-sine, span length between 12.5 and 100 m, and damping ratio between 0.25% and 2%. **DOI: 10.1061/(ASCE)BE.1943-5592.0001780**.

Introduction

Progressive use of light and strong construction materials and the development of innovative structural forms have resulted in an increasing number of beautiful footbridge structures that are quickly becoming city landmarks. Critical design considerations for these structures include vibration performance under dynamic loading generated by human walking (Racic and Brownjohn 2009).

Computational evaluation of vibration response often involves use of a modal model of the structure and a mathematical model of walking-induced dynamic force. The evaluation can be done either in the design stage or at the completion stage. In the design stage, there are large uncertainties in both the dynamic properties of the structure (e.g., natural frequency and damping ratio) and the loading parameters (e.g., walking frequency). The uncertainties can affect the reliability of the calculated responses. A practical solution in this stage is the use of design spectra, as proposed in some design recommendations such as BSI (2011) and HiVoSS (2008).

At the completion stage, the uncertainty in vibration response prediction can be reduced by measuring the dynamic properties of the structure. In addition, vibration responses to a limited number of walking scenarios (depending on time and cost) can be measured. A more detailed evaluation of vibration response for a number of relevant loading scenarios is then performed in the office, and used to decide whether vibration mitigation is required (Tubino et al. 2015). Under these circumstances, the reliability of the calculated responses depends mainly on the accuracy of the employed mathematical model for the dynamic loading.

The pedestrian models have evolved from simplistic harmonic force for an average walker to those that aim to capture variations in pedestrian's pacing frequency and/or dynamic force waveform for a relevant population of walkers (Zivanović et al. 2007; Racic and Brownjohn 2011; Krenk 2012; Younis et al. 2017). The new models are often so detailed to include not only main harmonics (at integer multiples of pacing frequency) but also the subharmonics that appear between the main harmonics owing to asymmetry of the human gait. The present authors have recently developed a model that accounts for first five harmonics and subharmonics and is the only model that accounts for variations in speed of pedestrian crossing the bridge (García-Diéguez et al. 2021).

Some of the recent models have been formulated in either a spectral load or a response spectrum format that is convenient for use in design (Wan et al. 2009; Brownjohn and Racic 2016; Wang et al. 2020; Van Nimmen et al. 2020). However, none of the proposals have yet been adopted by design guidelines for footbridges (Ricciardelli and Demartino 2015) owing to a lack of evidence of their comparative performance on as-built structures. In addition, relative importance of forcing parameters in response calculations is still debated and requires further in-depth research.

The aim of this paper is to: (1) perform sensitivity analysis to evaluate influence of variability in dynamic force and natural frequency of the structure on the vibration response; and (2) develop a response spectrum model as a means of quick insight into range of possible responses when all uncertainties of interest are considered.

To achieve these aims, an extensive database of numerically simulated responses to a single pedestrian's excitation was generated. Simulations were performed for pedestrians drawn from a population with predefined properties. The structures were modeled as simply supported beams (Fig. 1) having span length between 12.5 and 100 m, half-sine mode shape, fundamental

[1]Dept. of Construction and Manufacturing Engineering, Univ. of Oviedo, Campus de Gijón 7.1.19, 33203 Gijón, Spain (corresponding author). ORCID: https://orcid.org/0000-0002-8960-5190. Email: garciadmarta@uniovi.es

[2]Dept. of Construction and Manufacturing Engineering, Univ. of Oviedo, Campus de Gijón 7.1.21, 33203 Gijón, Spain.

[3]College of Engineering, Mathematics and Physical Sciences, Univ. of Exeter, Exeter EX4 4QF, UK.

Note. This manuscript was submitted on February 6, 2021; approved on June 28, 2021; published online on August 11, 2021. Discussion period open until January 11, 2022; separate discussions must be submitted for individual papers. This paper is part of the ***Journal of Bridge Engineering***, © ASCE, ISSN 1084-0702.

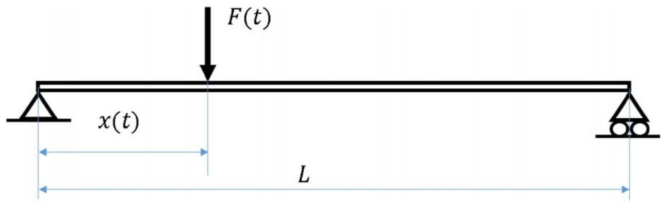

Fig. 1. Structure and load models.

vertical flexural natural frequency up to 10 Hz and damping ratio in the range 0.25–2%. A "complete statistical model" that accounts for walking speed variability as well as empirical correlations of other loading parameters with the speed (García-Diéguez et al. 2021) was employed to model pedestrians. This time domain model utilizes statistical description of the intrapedestrian and interpedestrian variabilities of the walking parameters on step-by-step basis. These parameters are: average speed (also referred to as step speed), duration (referred to as step interval), and dynamic load factors (DLFs) for the first five harmonics and subharmonics. Although other recent load models generally use the pacing frequency as an independent variable, the complete model has used the walking speed instead to reflect the fact that pedestrians aim to minimize the energy expenditure by optimizing walking speed (rather than pacing frequency) (Rose and Gamble 1994). At this stage, the model is developed for structures accommodating one walker at a time. It is known that footbridges might interact with pedestrians crossing them depending on the vibration frequency, response amplitude, and potentially duration of crossing time. As there are still no reliable models that can predict whether and under which conditions this interaction develops, the effects of potential interaction are neglected in this paper. This enables comparison of the model with the design spectra from the contemporary design guidelines, all of which neglect the interaction.

Extensive Monte Carlo simulations of the response were carried out for each structure configuration in the next section. The peak acceleration encountered at the midspan was chosen to quantify the individual responses. From the results, the response having 5% probability of exceedance was estimated and established as the characteristic response. The computed characteristic response was plotted in a spectrum format.

The obtained spectra are used in section "Sensitivity analysis" to study: (1) the influence of variability in the walking speed (which is not possible by using other models) and natural frequencies of the structures on the vibration responses; and (2) the importance of accounting for variability in the walking force when predicting the response. The spectra were modified in section "Design spectrum" to take into account the uncertainties of the mean walking speed of the pedestrian's population and the natural frequency of the structure arising at the design stage. Linear piecewise functions enveloping the modified spectra were adopted as the design spectra. The spectral amplitudes were defined as functions of the structural span and modal damping ratio. Finally, similarities and differences between the proposed spectra and those from a design guideline HiVoSS (2008) and a relevant British standard BSI (2008) were discussed.

Numerical Simulations

Structure Modeling

The structure was modeled as a single-span simply supported beam (Fig. 1) with constant cross section and span length, L, of 12.5, 25, 50, or 100 m. It was assumed that the fundamental flexural vibration mode is the main contributor to the vertical vibration response and that it can be modeled as a half-sine mode shape. The modal damping ratio, ξ, was chosen to cover structures from lightly (0.25% and 0.5%) to moderately damped (1% and 2%). The natural frequency was chosen to range from 0.5 to 10 Hz, in 0.1 Hz frequency increments. This results in a total of 1,536 structures.

The acceleration response $\rho(t)$ to a given dynamic load is calculated for a reference modal mass of 1 t (1,000 kg). Modal mass of 1 t is chosen for practical reasons, as it allows the actual response of a footbridge to be calculated having arbitrary modal mass by dividing the response read from the spectrum by the actual modal mass in "t" (thousands of kilograms).

Pedestrian Model

A dynamic load model for a pedestrian developed by the present authors and described in detail elsewhere (García-Diéguez et al. 2021) is used in the simulations. An overview of the model, however, is presented in this section for completeness of information. The vertical load generated while walking is modeled as a dynamic force whose both magnitude and position along the longitudinal axis of the structure vary in time (Fig. 1). Step speed, step interval, and DLFs for the first five harmonics and subharmonics are stochastic variables. Statistics of variations of these variables from one pedestrian to another (interpedestrian variability) and from one step to another for the same pedestrian (intrapedestrian variability) are included in the model. All variables are expressed as functions of the step speed. Their formulation is described in the following sections. The model was developed using measurements from 50 volunteers (from Spanish population) with a mean age of 42.1 years and standard deviation of 11.8 years, and therefore it is directly applicable to this and similar populations. The model could be adjusted to other populations once empirical data for those become available.

Step Speed

The step speed was modeled with the aim to reproduce the natural evolution of the walking speed as a pedestrian crosses the footbridge. Step speed v_i is defined here as the average speed in the ith step ($i = 1, 2, \ldots, N$), where N is the total number of steps required to cross the footbridge. The step speed is broken down into two components: $v_i = \bar{v} + \tilde{v}_i$, where $\bar{v}$ is a constant representing the interpedestrian component and $\tilde{v}_i$ is a random intrapedestrian component. Variable $\bar{v}$ is modeled using a Gaussian distribution $\bar{v} \sim N(\mu_v, \sigma_v)$ where μ_v and σ_v are the mean and standard deviation, respectively. They are taken to represent the normal walking recorded at three European locations: $\mu_v = 1.4$ and $\sigma_v = 0.14$ m/s (García-Diéguez et al. 2021).

It is worth noting that the value of the mean can vary from an application to another even for the same population, as the mean value is dependent on the actual usage of the structure, geographic location of the structure and, more generally, on "pace of life" (Kasperski and Sahnaci 2007). This uncertainty in the mean speed is taken into account in this paper by considering two additional values of $\mu_v = 1.54$ and $\mu_v = 1.26$ m/s, which correspond to fast and slow walking, respectively.

The random intrapedestrian component is described by a second-order autoregressive model $\tilde{v}_i = c_1\tilde{v}_{i-1} + c_2\tilde{v}_{i-2} + w_i$. The autoregressive parameters c_1 and c_2 are independent of the constant component, $\bar{v}$, and are statistically represented by a bivariate Gaussian distribution $\mathbf{C} \sim N_2(\mu, \Sigma)$ with the following mean μ and covariance Σ matrices:

$$\mu = \begin{bmatrix} 1.45 \\ -0.55 \end{bmatrix}, \quad \Sigma = \begin{bmatrix} 0.0210 & -0.0180 \\ -0.0180 & 0.0180 \end{bmatrix} \tag{1}$$

J. Bridge Eng., 2021, 26(10): 04021077

The disturbance w_i is modeled as Gaussian white noise $w_i \sim N(0, \sigma_w)$. The standard deviation of the disturbance, σ_w, is an interpedestrian parameter that does not depend on the value of $\bar{v}$. The experimental values of σ_w are within the interval [0, 1] and their histogram shows a unimodal shape. These features are adequately described by a Beta distribution, $B(17, 2103)$, whose parameters were identified by fitting the experimental data using the maximum likelihood method.

More details on step speed modeling can be found elsewhere (García-Diéguez and Zapico-Valle 2019).

Step Interval

For a given sequence of step speed, v_i, calculated in the previous section, the interval T_i of the ith step is broken down into two parts $T_i = \overline{T}_i + \widetilde{T}_i$, in which $\overline{T}_i$ is an adaptive part and $\widetilde{T}_i$ is a deviation. Here $\overline{T}_i$ represents the automatic adaptation of the gait to the walking speed. It is empirically formulated as a power law of the speed v_i in the corresponding step, $\overline{T}_i = c_3 v_i^{c_4 - 1}$. The parameters c_3 and c_4 vary from a pedestrian to another and are linearly correlated. The interpedestrian variability of these parameters is described by a bivariate Gaussian distribution $\mathbf{C} \sim N_2(\mu, \Sigma)$ having the following mean μ and covariance Σ matrices:

$$\mu = \begin{bmatrix} 0.586 \\ 0.463 \end{bmatrix}, \quad \Sigma = \begin{bmatrix} 0.0022 & -0.0015 \\ -0.0015 & 0.0062 \end{bmatrix} \qquad (2)$$

The deviation, $\widetilde{T}_i = \widetilde{T}_i^a + \widetilde{T}_i^r$, is composed of a deterministic part owing to the asymmetry of the gait, $\widetilde{T}_i^a$, and a random part, $\widetilde{T}_i^r$. The asymmetry part is formulated as $\widetilde{T}_i^a = c_{5i}(-1)^i$, in which c_{5i} is the asymmetry factor of the ith step that is expressed as a function of the adaptive part $c_{5i} = \overline{T}_i c_{n5}/2$. In this equation, c_{n5} stands for the normalized asymmetry parameter, which is considered to be constant in a footbridge crossing. The interpedestrian variability of this parameter follows a Beta distribution $c_{n5} \sim B(2.67, 149.10)$. The random part, $\widetilde{T}_i^r$, is described by a second-order autoregressive model $\widetilde{T}_i^r = c_{6i}\widetilde{T}_{i-1} + c_{7i}\widetilde{T}_{i-2} + z_i$, in which c_{6i} and c_{7i} are the autoregressive parameters and z_i is a random disturbance. Each autoregressive parameter is a second-order polynomial of the step speed, v_i, plus a random part: $c_{6i} = 0.0469\, v_i^2 - 0.0291\, v_i - 0.3448 + c_{n6}$ and $c_{7i} = -0.0370\, v_i^2 - 0.0122\, v_i - 0.1545 + c_{n7}$. The random parts, c_{n6} and c_{n7}, are independent of the step speed and their interpedestrian variabilities are described by symmetric Beta distributions: $c_{n6} \sim B(6.60, 6.60)$ and $c_{n7} \sim B(9.42, 9.42)$. The random disturbance of $\widetilde{T}_i^r$ is Gaussian white noise $z_i \sim \mathrm{N}(0, \sigma_{z_i})$. The standard deviation of the disturbances, σ_{zi}, is formulated as the product of two factors according to this equation: $\sigma_{z_i} = (v_i^2 - 3.30\ v_i + 3.00)c_8$. The first factor (in parentheses) represents the empirical trend with respect to the step speed, modeled as a second-order polynomial. The second factor, c_8, represents the interpedestrian variability of the standard deviation of the disturbances and it follows a Beta distribution $c_8 \sim B(14.15, 561.19)$.

The interpedestrian Gaussian distributions of the average walking speed in a footbridge crossing give rise to log-normal distributions of the average step frequency $f_s \sim \log N(\mu_f, \sigma_f)$ (García-Diéguez and Zapico-Valle 2019). The parameters of these distributions for three distributions of walking speed are listed in Table 1.

Position

The spatial position $\mathbf{x}$ of the walking force along the longitudinal axis of the footbridge is a function of time. As in other models for crossing the footbridge in noncrowded conditions, it is assumed that the pedestrian moves forward along a straight line parallel to the longitudinal axis. In addition, the variability in the speed is accounted for by approximating the position in the ith step as follows:

$$\mathbf{x}(t_i + \tau) = x_i + v_i \tau \quad (i = 1, 2, \ldots, N) \qquad (3)$$

where t_i and x_i are the time and position at the beginning of the step i, respectively, that are calculated as follows: $t_i = \sum_0^{i-1} T_i$, $x_i = \sum_0^{i-1} v_i T_i$, in which v_0 and T_0 are equal to zero. Here τ is time variable between 0 and T_i. All time domain variables are discretized at equally spaced time intervals $\Delta T = 0.001$ s in the numerical simulations. To avoid discontinuities in the force waveforms, the step intervals are rounded to integer multiples of ΔT.

Table 1. Parameters of the corresponding average walking speed and step frequency distributions

Walking speed	μ_v (m/s)	σ_v (m/s)	μ_f (Hz)	σ_f (Hz)
Fast	1.54	0.14	2.16	0.19
Normal	1.40	0.14	2.05	0.19
Slow	1.26	0.14	1.94	0.19

Table 2. Parameter values for the mean of DLF distribution

j	c_9	c_{10}	c_{11}	c_{12}	c_{13}
0.5	0.0049	−0.0028	0.0055	10.06	89.29
1	0.0037	0.3064	−0.1263	45.51	407.69
1.5	−0.0017	0.0222	0.0035	18.85	168.56
2	0.0341	−0.0551	0.0685	13.78	123.17
2.5	0.0077	−0.0140	0.0236	24.55	220.83
3	0.0118	−0.0246	0.0657	15.93	143.33
3.5	0.0114	−0.0270	0.0284	24.35	219.03
4	0.0103	−0.0039	0.0333	14.24	128.88
4.5	0.0077	−0.0164	0.0188	22.00	198.18
5	0.0024	0.0138	0.0089	10.66	96.85

Dynamic Load Factors

DLFs are labeled $\mathrm{DLF}_i^{(j)}$ in this paper. The subscript, $i = 1, 2, \ldots, N$, denotes the step number for the harmonics and stride number for the subharmonics, while the superscript denotes the order of the harmonics $j = 1, 2, \ldots, 5$ or subharmonics $j = 0.5, 1.5, \ldots, 4.5$. In a single footbridge crossing, $\mathrm{DLF}_i^{(j)}$ for each harmonic/subharmonic is a random variable that follows a Beta distribution $\mathrm{DLF}_i^{(j)} \sim B_i(a_i, b_i)$, in which a_i and b_i are the parameters of B_i that depends on the corresponding step/stride speed. These parameters are computed through the following functions of the mean $\mu_i^{(j)}$ and variance $(\sigma_i^{(j)})^2$ of B_i,

$$a_i^{(j)} = \frac{\left(\mu_i^{(j)}\right)^2\left(1 - \mu_i^{(j)}\right)}{\left(\sigma_i^{(j)}\right)^2} - \mu_i^{(j)}, \quad b_i^{(j)} = \frac{1 - \mu_i^{(j)}}{\mu_i^{(j)}} a_i^{(j)} \qquad (4)$$

The mean of the distribution in each step/stride is expressed as the product of two factors $\mu_i^{(j)} = \mu_{di}^{(j)} \cdot \mu_r^{(j)}$. The first factor corresponds to the gait adaptation to the step speed, which is formulated as a second-order polynomial $\mu_{di}^{(j)} = c_9^{(j)} v_i^2 + c_{10}^{(j)} v_i + c_{11}^{(j)}$. The second factor stays constant during a crossing. It represents the interpedestrian variability of the mean and it follows a Beta distribution $\mu_r^{(j)} \sim B(c_{12}, c_{13})$. The calibrated values of parameters c_9 to c_{13} are listed in Table 2.

J. Bridge Eng., 2021, 26(10): 04021077

The variance of the distribution is $(\sigma_i^{(j)})^2 = (\mathrm{CoV}_i^{(j)} \mu_i^{(j)})^2$ where the coefficient of variation, $\mathrm{CoV}_i^{(j)}$, is expressed as the product of two factors $\mathrm{CoV}_i^{(j)} = \mathrm{CoV}_{di}^{(j)} \cdot \mathrm{CoV}_r^{(j)}$. The first factor corresponds to the adaptation of the gait to the step speed, which is formulated as a second-order polynomial $\mathrm{CoV}_{di}^{(j)} = c_{14}^{(j)} v_i^2 + c_{15}^{(j)} v_i + c_{16}^{(j)}$. The second factor is constant in each crossing. It represents the interpedestrian variability of the CoV and it is modeled as a Beta distribution $\mathrm{CoV}_r^{(j)} \sim B(c_{17}, c_{18})$. The calibrated values of parameters c_{14} to c_{18} are listed in Table 3.

Force Synthesis

Pedestrian's weight W is modeled as a Gaussian distribution with a mean of 750 N and a standard deviation of 150 N, which are based on our previous experimental studies (García-Diéguez and Zapico-Valle 2017). As it is assumed that the structural response is dominated by a single mode of vibration, the relative phases of the force harmonics/subharmonics have a negligible effect on the response and are set to zero. The total force in the ith step consisting of the contribution of the five harmonics can be written as

$$\mathbf{F}^h(t_i + \tau) = W \sum_{j=1,2,3,4,5} \mathrm{DLF}_i^{(j)} \sin\left(\frac{2\pi j}{T_i}\tau\right) \quad (i = 1, 2, \ldots, N) \tag{5}$$

in which t_i denotes the time at the beginning of the step, $t_i = \sum_0^{i-1} T_i$ and $T_0 = 0$, τ is between 0 and T_i. The total force in the kth stride consisting of the contribution of the five subharmonics can be written as

$$\mathbf{F}^s(t_k + \tau) = W \sum_{j=0.5,1.5,2.5,3.5,4.5} \mathrm{DLF}_k^{(j)} \sin\left(\frac{2\pi 2j}{T_{2k-1} + T_{2k}}\tau\right) \times \left(k = 1, 2, \ldots, \frac{N}{2}\right) \tag{6}$$

in which t_k denotes the time at the beginning of the stride, $t_k = \sum_0^{2k-2} T_i$ and $T_0 = 0$, τ is between 0 and $(T_{2k-1} + T_{2k})$. With this formulation the walking force trace does not exhibit any discontinuity of first kind and the total force impulse in a stride is zero. The final force time history is equal to the sum of harmonic and subharmonic components and the pedestrian's weight: $\mathbf{F}(t) = \mathbf{F}^h(t) + \mathbf{F}^s(t) + W$. The number of steps, N, was selected long enough to cover the maximum span length of 100 m considered in the simulations. A summary of calculating the force and the corresponding position time histories for individual pedestrians is shown in Fig. 2.

Table 3. Parameter values for the CoV of DLF distribution

j	c_{14}	c_{15}	c_{16}	c_{17}	c_{18}
0.5	0	0	0.1000	13.53	12.10
1	0.1450	−0.4773	0.4625	13.35	121.81
1.5	0	0	0.1000	27.33	24.54
2	0	0	0.1000	7.90	12.82
2.5	0	0	0.1000	39.65	36.29
3	0	0	0.1000	5.73	12.67
3.5	0	0	0.1000	23.24	19.41
4	0	0	0.1000	5.04	13.73
4.5	0	0	0.1000	20.53	16.62
5	0	0	0.1000	5.12	10.56

Integration and Characterization of Responses

A total of 10,000 force and the corresponding position time histories were generated for each of the three populations of pedestrians (associated with the three speed distributions analyzed). The response of 1,536 footbridges to all generated walking forces was obtained in the modal space by using the following procedure. First, the force was weighted by the mode shape to calculate the corresponding modal force. The modal force was then transformed to the frequency domain by the fast Fourier transform (FFT). The acceleration response in the frequency domain was obtained by multiplying the load by the structure's accelerance. This acceleration response was then converted to the time domain, $\mathbf{a}(t)$, using the inverse FFT. This resulted in computing a total of 46.08 million responses.

Each response was quantified through its peak acceleration value $a_p = \max(|\mathbf{a}(t)|)$. The 10,000 peak accelerations corresponding to each structure configuration and walking speed distribution were sorted in ascending order $a_{p1:10,000} \leq a_{p2:10,000} \leq \cdots \leq a_{p10,000:10,000}$. Finally, the characteristic acceleration response ρ_{95} having 5% probability of exceedance was estimated from the 9,500:10,000 order statistic $\rho_{95} = a_{p9,500:10,000}$. This value, expressed in t m/s^2, was used for development of the response spectra.

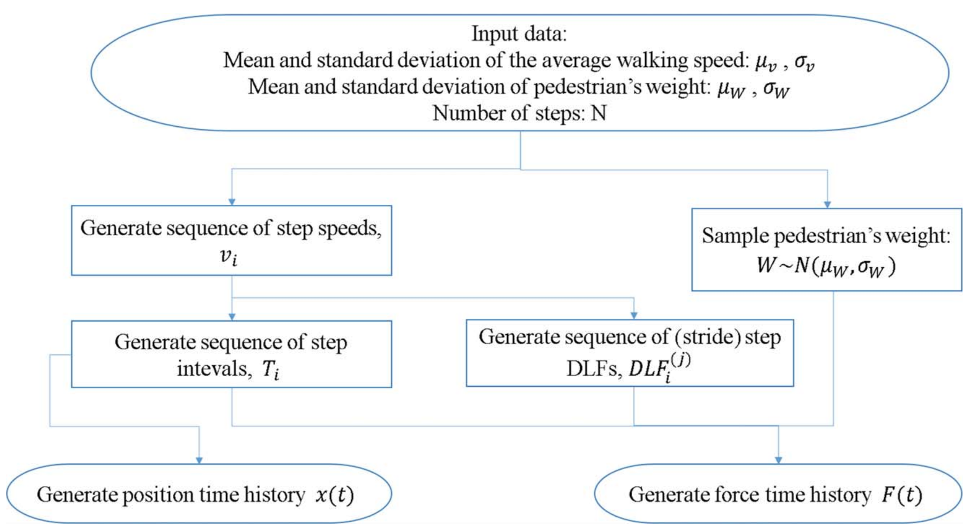

Fig. 2. Flow chart for calculating the force.

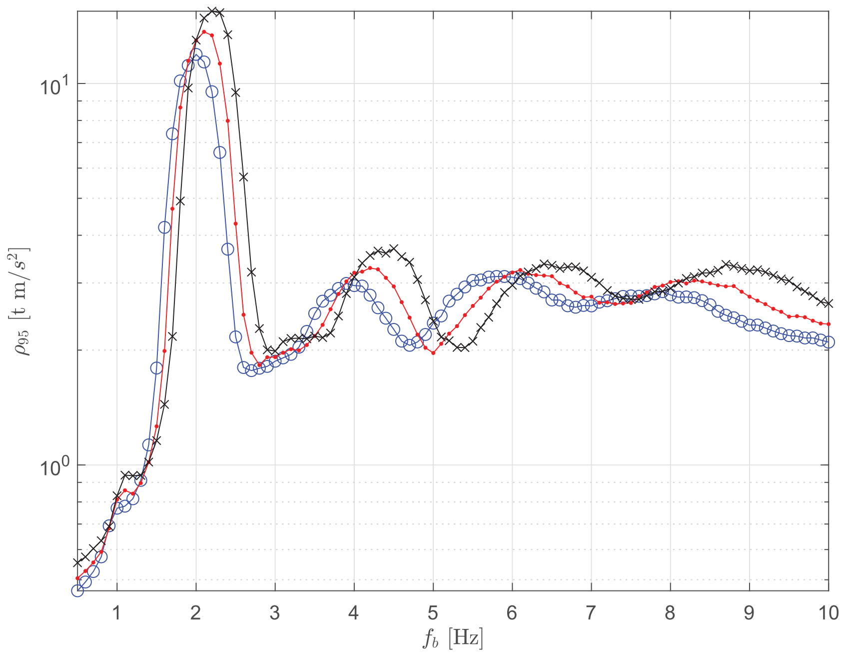

Fig. 3. Response spectra for $L = 50$ m and $\xi = 0.5\%$. ○ = slow walking; • = normal walking; × = fast walking.

The defined characteristic acceleration response corresponds to the reference modal mass of 1 t, as explained previously.

Sensitivity Analysis

Influence of Mean Walking Speed and Structural Frequency on Vibration Response

The response spectra of a structure having $L = 50$ m and $\xi = 0.5\%$ for the three considered distributions of walking speed are shown in Fig. 3.

All spectra exhibit the highest peak at the fundamental harmonic of the walking load. These peaks occur at frequencies that are slightly higher than the means of the corresponding step frequency distributions (Table 1). There are also other lower and broader peaks at the higher harmonics. The peaks corresponding to the first two subharmonics are also visible and their magnitude is lower than those of the main harmonics. The effects of higher subharmonics are not noticeable as they are masked by those of the harmonics. The shape of the obtained spectra is similar to those developed for predicting floor vibration (Brownjohn and Racic 2016). Fig. 3 shows that an increase in the mean speed shifts the spectrum up and to the right. To quantify the effect that the mean speed value has on the response, the relative difference in the reference response with respect to that corresponding to normal walking was calculated at each footbridge frequency. Results are shown in Fig. 4.

Deviations are both positive and negative. The extreme deviations are in the range of the fundamental harmonic of the walking load (1.5–2.5 Hz) and reach values as high as +130% and −54%. Outside this zone, the deviations are lower and they range between +40% and −22%. Results demonstrate that the response is extremely sensitive to the parameters of the walking speed distribution, confirming the findings elsewhere in the literature (Pedersen and Frier 2010). This is due to the fact that in our model the distribution of step speed, in turn, influences the distribution of step frequency and DLFs. Faster speed generally results in higher pacing rate and larger DLFs, which is why resonance in the spectra moves to the right and increases in magnitude in Fig. 3.

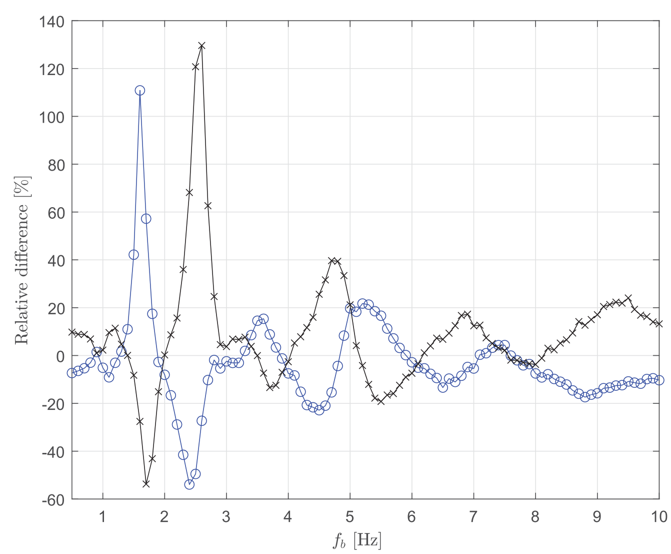

Fig. 4. Difference relative to the normal walking response spectrum for $L = 50$ m and $\xi = 0.5\%$. ○ = slow walking; × = fast walking.

The natural frequency of the structure can be estimated either by using empirical formulas for typical structure configurations or from modal analysis of finite element model of the structure. In both cases there will be inevitable differences between the predicted and actual values of this parameter. A comparison between results of in situ experiments and refined finite element models of eight footbridges show that relative difference (calculated with respect to the measured frequency) is typically up to 10% (Van Nimmen et al. 2014). The influence of this uncertainty in the predictions of the response has been studied as in the previous section. Fig. 5 shows the response spectrum of the same structure having $L = 50$ m and $\xi = 0.5\%$ corresponding to normal walking and the original frequency. The uncertainty in the natural frequency was taken into account by translating the spectrum back and forth by 10% of the original natural frequency. The translated spectra are also shown in Fig. 5 for comparison purposes.

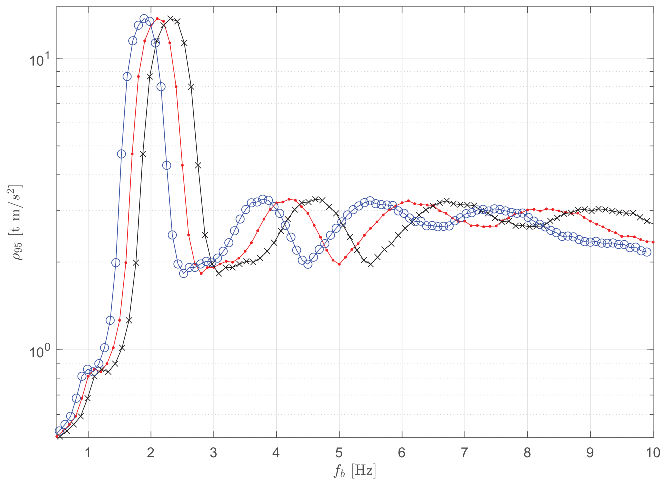

Fig. 5. Response spectra for $L = 50$ m and $\xi = 0.5\%$ and normal walking. ○ = original frequency × 0.9; • = original frequency; × = original frequency × 1.1.

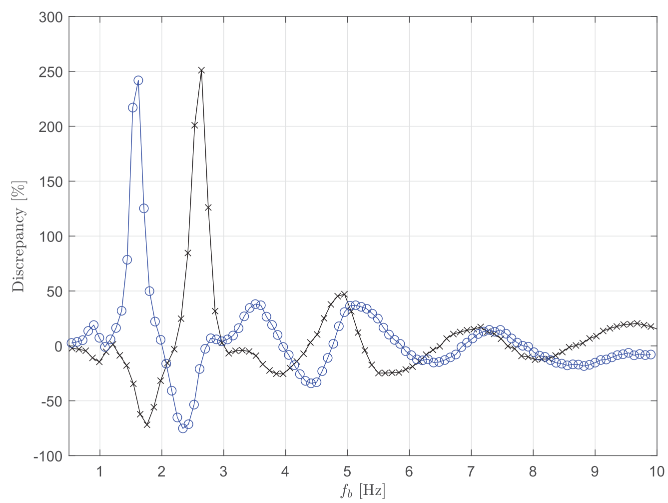

Fig. 6. Difference relative to the original spectrum for $L = 50$ m and $\xi = 0.5\%$. ○ = original frequency × 0.9; × = original frequency × 1.1.

The discrepancies of the responses corresponding to the translated spectra with respect to the original were quantified at each footbridge frequency through their relative difference. Results are shown in Fig. 6. Overall, the discrepancies have a similar distribution and are even higher than those of the mean speed. In this case, the largest deviations are in the range of the walking frequency (1.5–2.5 Hz) and they range from +251% to −75%. Outside this zone, the deviations are between +47% and −34%. The results show that both speed and natural frequency uncertainties should be considered at the design stage to obtain actual range of possible vibration responses.

Performance of Dynamic Force Models of Various Complexity

It is assumed in this section that the properties of the structure and walking loads are known. The capability of different loading models to predict the vibration response is analyzed. The structure used here is the same as in the previous section, i.e., $L = 50$ m and $\xi = 0.5\%$ and a modal mass of 1 t. Three models with decreasing level of complexity are considered: complete statistical model,

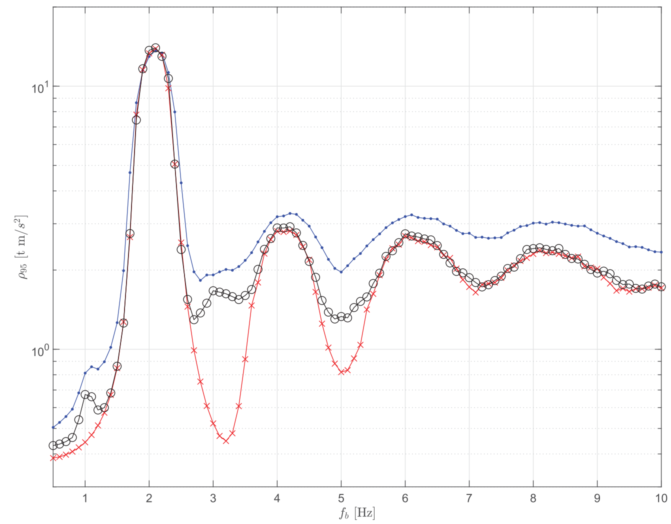

Fig. 7. Response spectra for $L = 50$ m, $\xi = 0.5\%$, and normal walking. • = complete load model; ○ = periodic load model; × = periodic-without-subharmonics load model.

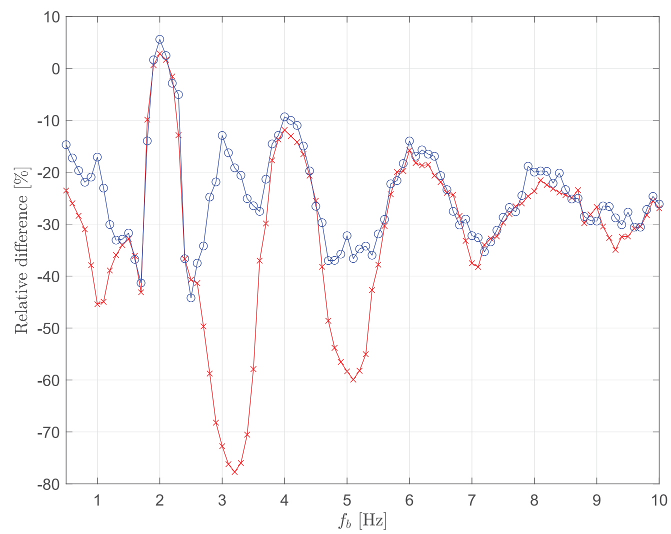

Fig. 8. Difference relative to the complete load model spectrum for $L = 50$ m, $\xi = 0.5\%$, and normal walking. ○ = periodic load model; × = periodic-without-subharmonics load model.

periodic model and periodic-without-subharmonics model. The complete statistical model is that defined previously. The periodic model was obtained from the complete model by setting all the step variables constant and equal to their mean values: $v_i = \overline{v}$, $T_i = c_3 \overline{v}^{c_4 - 1}$ and $\mathrm{DLF}_i^{(j)} = \mu_i^{(j)} = (c_9^{(j)} \overline{v}^2 + c_{10}^{(j)} \overline{v} + c_{11}^{(j)}) \cdot \mu_r^{(j)}$. Thus, the walking load becomes a periodic function. The periodic-without-subharmonics model was obtained from periodic model by excluding contribution of the subharmonics to the forcing function.

The response spectra were recalculated by applying the periodic model and the periodic-without-subharmonics model to the normal walking. The spectra are depicted in Fig. 7 along with that of the complete model for comparison purposes. The differences of the spectral ordinates corresponding to both models relative to those of the complete model are shown in Fig. 8. It can be seen that the periodic model slightly overestimates (up to 5%) the actual characteristic response within a narrow range 1.85–2.15 Hz around the mean of the step frequency distribution, 2.05 Hz (Table 1), i.e., when the resonance response is excited by the first harmonic. Outside this range, the periodic model underestimates the characteristic response by as much as 44%. A possible explanation of this outcome is that intrapedestrian variability of the higher harmonics is nearly four times higher than that of the fundamental harmonic (García-Diéguez et al. 2021).

The shape of the spectrum of the periodic-without-subharmonics model is similar to that of the periodic model except at footbridge frequencies excited by the first three subharmonics. Neglecting the contribution of the subharmonics in the periodic model gives rise to underestimations of the spectral response by up to 78%. Fig. 7 shows that the response corresponding to the second and third subharmonics is around $2\,t\,\text{m/s}^2$ and those of the higher-order harmonics are just above $3\,t\,\text{m/s}^2$. The response corresponding to the second and third subharmonics has therefore the same order of magnitude as that of the higher harmonics, demonstrating the importance of including the subharmonics in force modeling. In addition, future expansion of the model to the crowd loading will require accurate description of the full frequency content of the forcing function to improve vibration assessment under cumulative effects of multiple pedestrians.

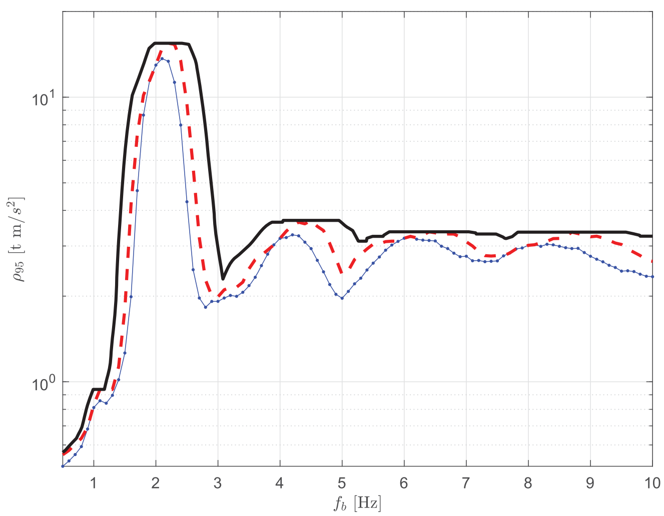

Fig. 9. Response spectra for $L = 50$ m, $\xi = 0.5\%$. ● = normal walking spectrum; dashed line = envelope spectrum; bold line = modified spectrum.

Design Spectrum

Consideration of Uncertainties

The estimation of structure and load variables at the design stage contains uncertainties that can significantly affect the predicted value of the response. This section proposes a way to account for the uncertainties in two key variables: mean walking speed and natural frequency of the structure.

It was demonstrated in the previous section that the response is very sensitive to the mean speed of the pedestrians. Unfortunately, this parameter varies from one application to another. Therefore, a certain difference between the predicted and actual mean speed is expected in practice. A conservative strategy is established to overcome this problem. Instead of using a fixed value for the mean speed, all of fast, normal, and slow walking were considered in the simulations. The envelope of the three considered spectra is then adopted for the design spectrum. Fig. 9 shows the spectrum (dashed line) that envelops the spectra for three speeds for $L = 50$ m, $\xi = 0.5\%$ footbridge. The spectrum for the normal walking speed is also shown (solid line with dot markers) in the same figure. For context, the spectra for fast and slow walking can be seen in Fig. 3. The envelope spectrum ensures that the characteristic value of the response for a footbridge is estimated assuming most conservative mean value of the population's speed of walking (i.e., the speed that ensures highest incidence of resonance and/or near-resonance responses for a structure analyzed).

The high influence of the uncertainty in the estimation of the natural frequency of the structure was demonstrated in the previous section. This uncertainty is taken into account by translating the envelope

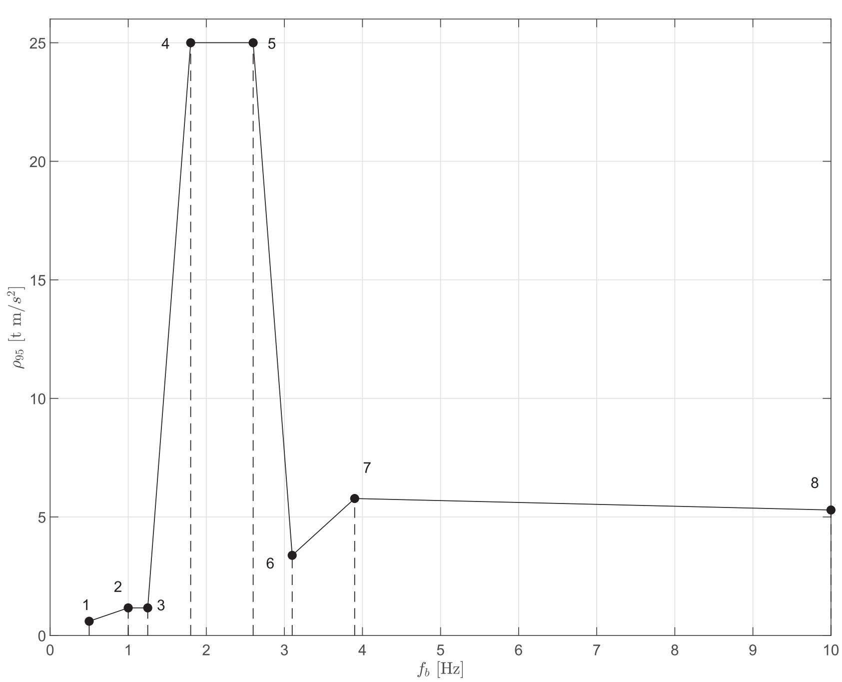

Fig. 10. Design spectrum for $L = 100$ m and $\xi = 0.25\%$.

spectrum back and forth for the 10% of the initially estimated value of the natural frequency. The resulting spectrum enveloping the initial and the two translated spectra represents the final "modified spectrum." Such a spectrum for a $L = 50$ m, $\xi = 0.5\%$ footbridge is shown as a solid black line in Fig. 9. This figure shows widening of the peak that corresponds to the first harmonic of walking load in the modified spectrum and almost flat value of the spectrum for vibration modes with natural frequencies above 4 Hz.

Modeling

Piecewise linear functions were chosen for the design spectrum. This function is easy to apply in practice and it is found to fit well the modified spectra corresponding to all considered structure configurations. The shape of the design spectrum is defined by eight points, whereby two successive points are connected by a linear segment, as shown in Fig. 10.

The abscissae f_v for these eight points are at 0.5, 1.0, 1.25, 1.8, 2.6, 3.1, 3.9, and 10.0 Hz. The parameters that are used to define the eight ordinates are listed in Table 4.

The characteristic ordinates of the vertices (in $t\,\text{m/s}^2$), ρ_{95}, are formulated as functions of the structure length L (in m):

$$\rho_{95} = A_1 \ln(L) + A_2 \quad (7)$$

Table 4. Parameter of the complete design spectrum

Vertex	f_v (Hz)	A_{11}	A_{12}	A_{13}	A_{21}	A_{22}	A_{23}
1	0.5	0	0	0	0	0	0.600
2	1.0	0.0087	−0.0606	0.10385	−0.0302	0.1520	0.4913
3	1.25	0.0087	−0.0606	0.1038	−0.0302	0.1520	0.4913
4	1.8	0.6996	−2.6829	2.4973	−2.3697	4.5072	0.9850
5	2.6	0.6996	−2.6829	2.4973	−2.3697	4.5072	0.9850
6	3.1	0.0802	−0.2398	0.2834	−0.2801	0.2307	0.6923
7	3.9	0.1812	−0.4483	0.4275	−0.5374	0.3818	0.9043
8	10.0	0.1751	−0.3202	0.2896	−0.4319	−0.0500	1.1253

Here A_1 and A_2 are defined as functions of the damping ratio of the structure, ξ, expressed as a percentage:

$$A_1 = A_{11}(\ln(\xi))^2 + A_{12}\ln(\xi) + A_{13}$$
$$A_2 = A_{21}(\ln(\xi))^2 + A_{22}\ln(\xi) + A_{23} \quad (8)$$

Thus, the response is formulated as a function of both structure length and damping ratio. Parameters A_1 and A_2 corresponding to each vertex and damping ratio were obtained by fitting Eq. (7) to the values of the response, ρ_{95}, calculated for each length, L, by the least squares method. Then, parameters (A_{11}, A_{12}, A_{13}) and (A_{21}, A_{22}, A_{23}) were computed by fitting Eq. (8) to the calculated values of A_1 and A_2 for each damping ratio, respectively, by the least squares method. The deviations of responses predicted by Eq. (7) with respect to the calculated responses were in all configurations within the interval ±4%, which indicates highly satisfactory match between the proposed model to the calculated responses. The fitted curves along with the results of the simulations are depicted in Fig. 11 for vertex 7. Fig. 11 shows that the curves have an adequate trend to reproduce the calculated responses.

Fig. 12 shows the proposed design spectra for four of the considered structure configurations superimposed on the calculated spectra. In all cases the design spectra depict the calculated ones closely.

To estimate the response for a given frequency of the structure requires linear interpolation between the anterior and posterior vertices of the design spectrum. The characteristic acceleration response is obtained by dividing the response read from the spectrum by the actual modal mass of the structure $a_{95} = \rho_{95}/m$, in which m is expressed in "t" (thousands of kilograms).

Comparison with Other Proposals

The method proposed here for checking the limit state of vibrations is now compared with those recommended by the British Standard Institution (BSI 2008) and the Human induced Vibrations of Steel Structures (HiVoSS) project (HiVoSS 2008). Annex A of BSI (2011) contains recommendations on vibration serviceability for foot and cycle bridges. In section A.4 of BSI (2011), a simplified

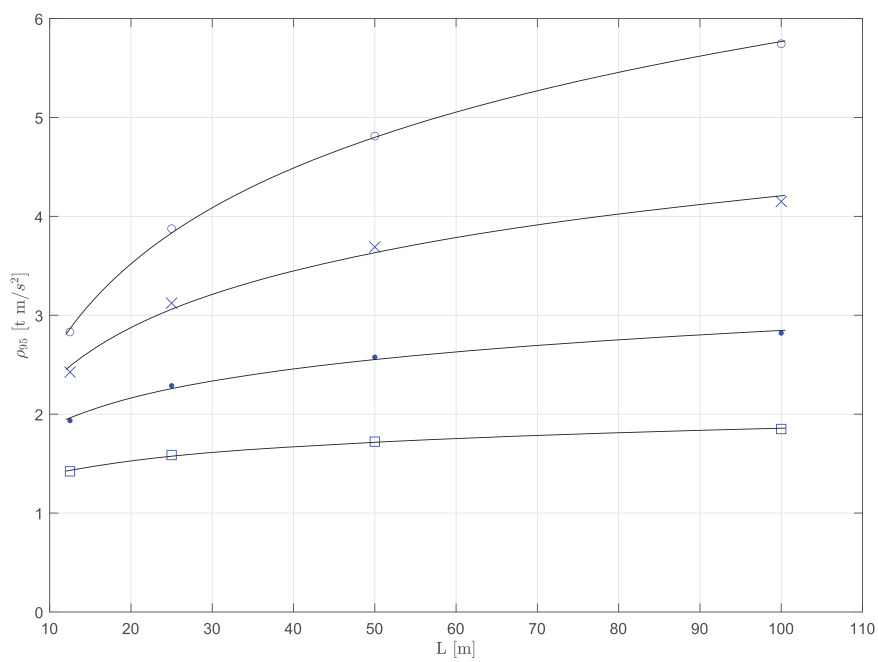

Fig. 11. Response at vertex 7 as a function of structure length, L and damping ratio ξ. Lines: predictions of the proposed function. Marks = results of simulations; ○ = $\xi = 0.25\%$; × = $\xi = 0.5\%$; • = $\xi = 1\%$; □ = $\xi = 2\%$.

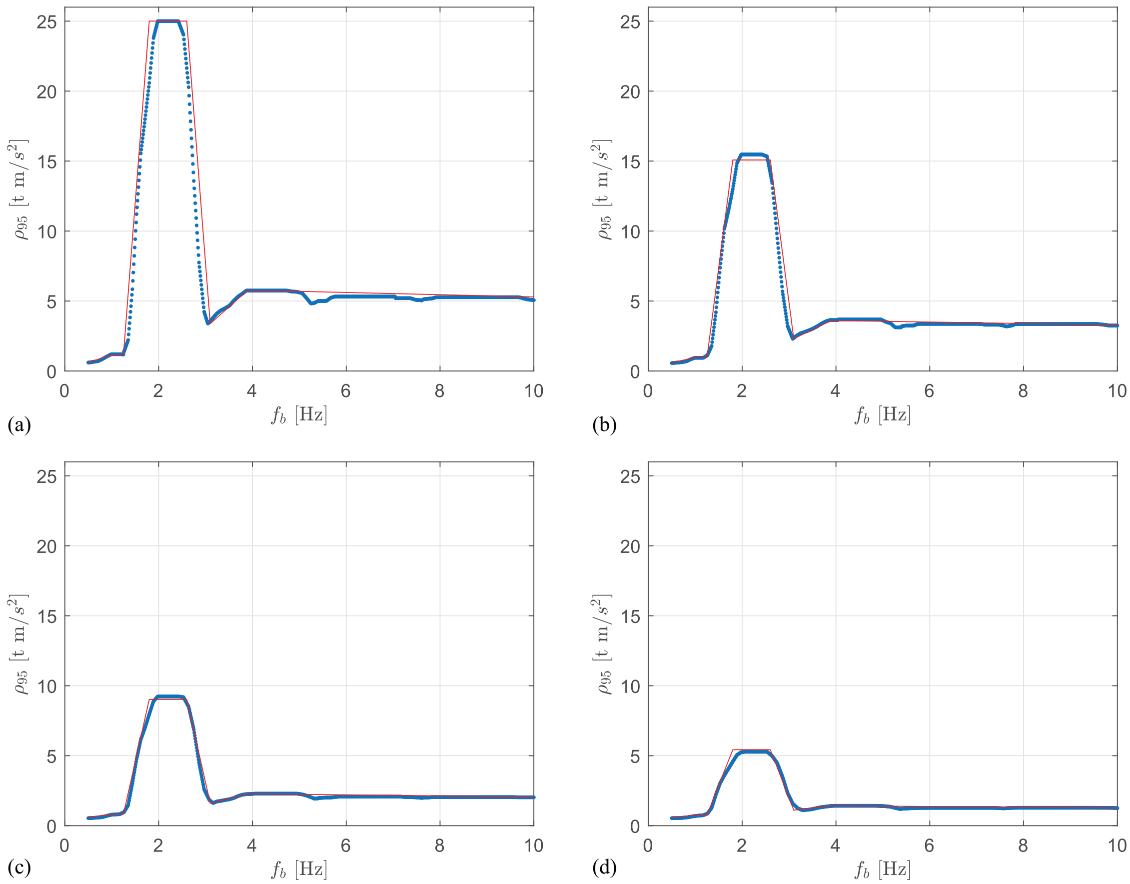

Fig. 12. Spectra for different configurations: (a) $L = 100$ m and $\xi = 0.25\%$; (b) $L = 50$ m and $\xi = 0.5\%$; (c) $L = 25$ m and $\xi = 1\%$; and (d) $L = 12.5$ m and $\xi = 2\%$. Dots = modified spectra; line = design spectra.

method is proposed for deriving the maximum vertical acceleration owing to a single pedestrian and pedestrian groups. As in our proposal, this method can be applied to simply supported structures of constant cross section under unrestricted walking traffic. The acceleration is formulated as a function of the footbridge length, L, and the modal damping expressed as the logarithmic decrement of decay of vibration, δ. The graphic is similar to that of Fig. 11. The amplitude of the walking load is defined in BSI (2008) as a product of two factors. The first factor is the reference load, which is set to 280 N. The second factor is a function of the structure frequency and it accounts for the probability of exciting structure resonance and the attenuation of amplitude for higher harmonics. It is defined graphically in the interval 0–8 Hz by means of functions with bell-like shapes that cover the frequency range of the first three forcing harmonics.

HiVoSS (2008) proposed a similar design procedure, drawing on the inspiration from the field of wind engineering. It is applicable to footbridges of constant cross section and having sinusoidal modal shape. The method is based on Monte Carlo time domain simulations of footbridges with spans in the range 20–200 m. The characteristic vertical acceleration is formulated as a function of the amplitude of the walking load, the modal mass of the structure, and a dynamic response factor. The dynamic response factor is defined empirically as a function of modal damping ratio, ξ. The amplitude of the walking load is also defined as the product of two factors. As in the previous case, the first factor is the load amplitude of an "average" pedestrian, which is set to 280 N, and the second factor is a function of the structure frequency. The latter is defined as a set of linear piecewise functions that cover the frequency range up of the first two harmonics (i.e., up to about 5 Hz).

Table 5. Properties of the considered footbridges

Case	L (m)	δ	ξ (%)
(a)	50	0.03	0.477
(b)	50	0.05	0.796
(c)	25	0.03	0.477
(d)	25	0.05	0.796
(e)	12.5	0.03	0.477
(f)	12.5	0.05	0.796

The two design methods are based on premises similar to those established in the method described in this paper, creating an opportunity to make a direct comparison. For this purpose, the response spectrum was computed for six different cases. They are detailed in Table 5 and the results are depicted in Fig. 13.

There are significant differences between the spectra proposed in this study and the corresponding spectra of HiVoSS and BSI. HiVoSS spectra show the greatest differences. This is because the influence of the length of the structure is not considered in the formulation of the dynamic response factor. Thus, HiVoSS predictions are lower for large spans and they are higher for short spans. The first peaks of the BSI spectra are similar to those proposed here. However, they are shifted by around 0.4 Hz. The first peaks of the HiVoSS spectra are narrower than those proposed here and they are also shifted by around 0.4 Hz. These shifts are due to differences in the pedestrian load model, to which the response is proportional. Both BSI and HiVoSS consider the load amplitude to be constant, whereas in our model the load amplitude is variable and it replicates the population rather than "average" individual. The load amplitude and response for pacing rates below 2 Hz, which is the typical value, are

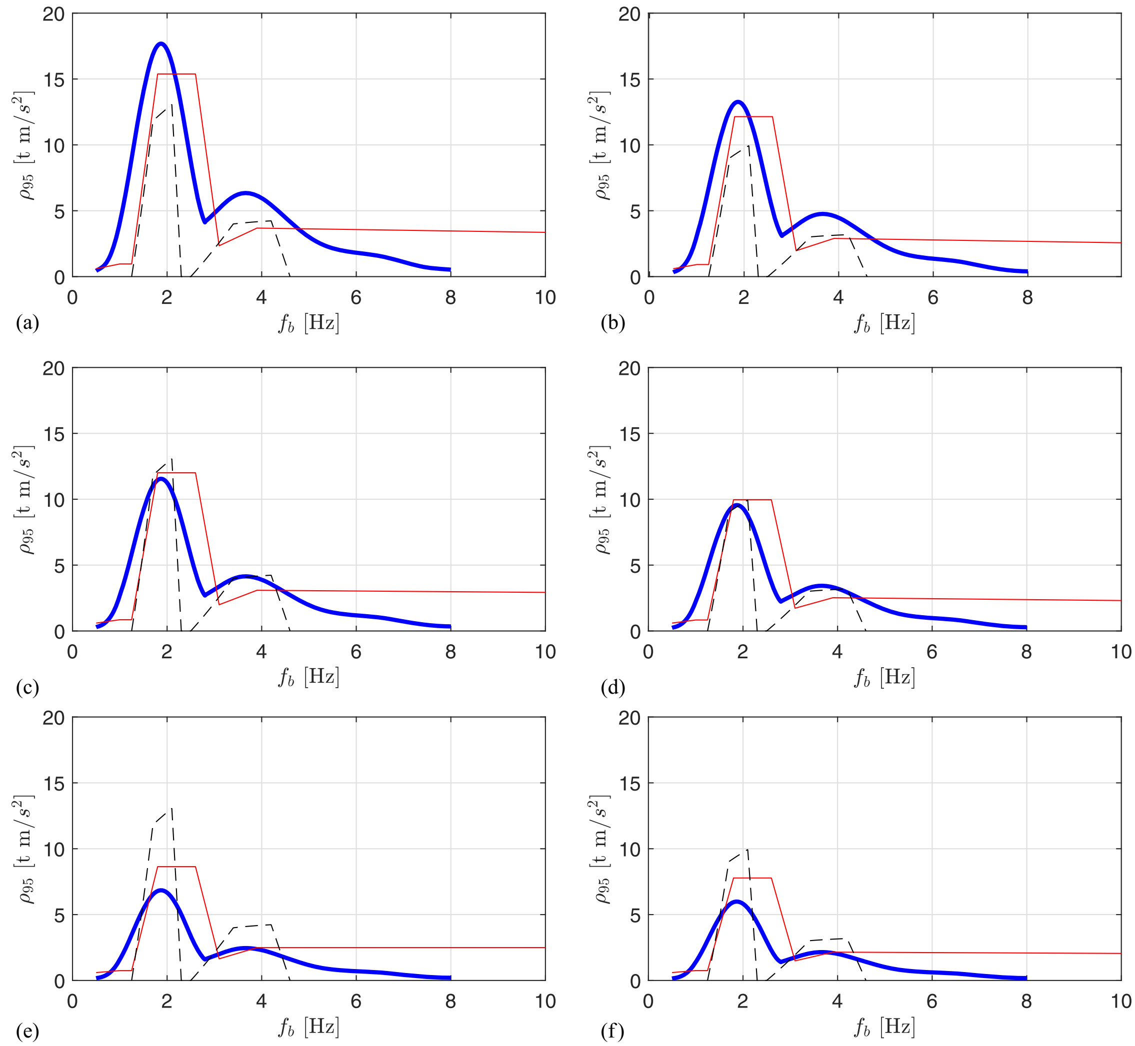

Fig. 13. Response spectra for cases (a)–(f) defined in Table 5. Fine line: present method. Bold line: BSI method. Dashed line: HiVoSS method.

lower in our model. Conversely, they are higher for pacing rates above 2 Hz. Both BSI and HiVoSS predict higher responses for the second peak. The response beyond 4 Hz predicted by the proposed method is significant and almost constant. HiVoSS does not consider the response above about 4.5 Hz whereas the BSI response is lower. This could prove a challenge for applying BSI and HiVoSS design approaches for evaluating vibration serviceability of increasingly lightweight footbridges, such as those made of aluminum and fiber-reinforced polymer composites, which are often responsive to higher harmonics of the walking-induced dynamic loading (Dey et al. 2016; Russell et al. 2020). An illustration of dynamic properties typical of lightweight FRP structures is available in a recent review paper. Wei et al. (2019) reported that seven FRP footbridges having main span between 15 and 63 m, had fundamental vertical natural frequency between 1.0 and 7.5 Hz, and damping ratio between 0.4% and 2.6%. The modal mass was available for three of these structures: it included an average (per meter area of the deck) modal mass as low as about 20 kg/m^2 and as large as 105 kg/m^2.

Conclusions

The sensitivity analysis carried out on common-span footbridges has revealed that the calculated dynamic response is sensitive to the uncertainties in both mean walking speed and natural frequency that arise in the design stage. Accommodating variations in the two parameters alters the vibration response up to 130% and 251%, respectively. Consequently, the uncertainties in the modal properties of the structure and the parameters of the interpedestrian distribution of walking speed should be considered at the design stage to provide insight into potential vibration response range should the pedestrian and structure properties differ from those assumed/calculated at the first instance. These results also emphasize the need for future extensive field observations that will allow a better understanding of actual walking speed and its potential relationship with the structure purpose or location.

In addition, the vibration response was found to be sensitive to the simplifications in the load modeling. Periodic models of walking forces give rise to errors in the prediction of the response up to 44%. If the subharmonics are further excluded from the load model, the error is up to 78%. Therefore, a model that reflects the narrowband nature of the forcing function around its both main harmonics and subharmonics should be used when evaluating the vibration serviceability state.

A linear piecewise design spectrum for assessing the vibration response to single-pedestrian traversing a simply-supported low-frequency structure has been developed in this paper. The ordinates of the vertices of this function were formulated as functions of the structure length and modal damping ratio. Comparison with related design spectra recommended in contemporary design codes and guidelines showed significant discrepancies. More importantly, it has been shown that uncertainties that are present at the design stage lead to poor ability to predict the vibration response with confidence, until some or all uncertainties are removed. As removal of uncertainties from the design is unrealistic expectation, we predict an increase in demand for routine testing of newly built structures and implementation of vibration suppression measures, if required. This is especially so as new structures, such as those made from fiber-reinforced polymer composites or aluminum, are becoming even more slender and lighter than in the past two decades.

Data Availability Statement

Some or all data, models, or code that support the findings of this study as well as simulation results (Matlab) used in sections "Sensitivity analysis" and "Design spectrum" are available from the corresponding author upon reasonable request.

Acknowledgments

The authors would like to acknowledge the financial support provided by the Spanish Ministry of Economy and Competitiveness through project PGC2018-096670-B-I00. The authors also would like to thank all the volunteers for their generous help in obtaining the experimental data used in this study.

References

Brownjohn, J.-M.-W., and V. Racic. 2016. "Universal response spectrum procedure for predicting walking-induced floor vibration." *Mech. Syst. Sig. Process.* 70 (22): 741–755. https://doi.org/10.1016/j.ymssp.2015.09.010.

BSI (British Standards Institution). 2008. "UK National Annex to Eurocode 1: Actions on Structures-Part 2: Traffic Loads on Bridges." London: BSI.

BSI (British Standards Institution). 2011. "Background to the National Annex to BS en 1991-2. Traffic loads on bridges." London: BSI.

Dey, P., A. Sychterz, S. Narasimhan, and S. Walbridge. 2016. "Performance of pedestrian-load models through experimental studies on lightweight aluminum bridges." *J. Bridge Eng.* 21 (8): C4015005. https://doi.org/10.1061/(ASCE)BE.1943-5592.0000824.

García-Diéguez, M., V. Racic, and J.-L. Zapico-Valle. 2021. "Complete statistical approach to modelling variable pedestrian forces induced on rigid surfaces." *Mech. Syst. Sig. Process.* 159 (3): 107800.

García-Diéguez, M., and J.-L. Zapico-Valle. 2017. "Statistical modeling of the relationships between spatiotemporal parameters of human walking and their variability." *J. Struct. Eng.* 143 (12): 4017164. https://doi.org/10.1061/(ASCE)ST.1943-541X.0001899.

García-Diéguez, M., and J.-L. Zapico-Valle. 2019. "Statistical modelling of spatiotemporal variability of overground walking." *Mech. Syst. Sig. Process.* 129 (1): 186–200.

HiVoSS (Human induced vibration of steel structures). 2008. "Research fund for coal and steel." *Design of Footbridges, Technical report*, Brussels: RFCS publications. https://doi.org/10.2777/79056.

Kasperski, M., and C. Sahnaci. 2007. "Serviceability of pedestrian structures." In *Proc., IMAC XXV*. Society for Experimental Mechanics Series, 2: 774–798. Bethel, Conn: Society for Experimental Mechanics.

Krenk, S. 2012. "Dynamic response to pedestrian loads with statistical frequency distribution." *J. Eng. Mech.* 138 (10): 1275–1281. https://doi.org/10.1061/(ASCE)EM.1943-7889.0000425.

Pedersen, L., and C. Frier. 2010. "Sensitivity of footbridge vibrations to stochastic walking parameters." *J. Sound Vib.* 329 (13): 2683–2701. https://doi.org/10.1016/j.jsv.2009.12.022.

Racic, V., and J.-M.-W. Brownjohn. 2009. "Experimental identification and analytical modelling of human walking forces: Literature review." *J. Sound Vib.* 326 (1–2): 1–49. https://doi.org/10.1016/j.jsv.2009.04.020.

Racic, V., and J.-M.-W. Brownjohn. 2011. "Stochastic model of near-periodic vertical loads due to humans walking." *Adv. Eng. Inf.* 25 (2): 259–275. https://doi.org/10.1016/j.aei.2010.07.004.

Ricciardelli, F., and C. Demartino. 2015. "Design of footbridges against pedestrian-induced vibrations." *J. Bridge Eng.* 21 (8): C4015003.

Rose, J., and J. Gamble. 1994. *Human walking*. Philadelphia: Williams & Wilkins.

Russell, J., X. Wei, S. Živanović, and C. Kruger. 2020. "Vibration serviceability of a GFRP railway crossing due to pedestrians and train excitation." *Eng. Struct.* 219: 110756. https://doi.org/10.1016/j.engstruct.2020.110756.

Tubino, F., L. Carassale, and G. Piccardo. 2015. "Human-induced vibrations on two lively footbridges in Milan." *J. Bridge Eng.* 21 (8): C4015002.

Van Nimmen, K., G. Lombaert, G. De Roeck, and P. Van den Broeck. 2014. "Vibration serviceability of footbridges: Evaluation of the current codes of practice." *Eng. Struct.* 59 (1–2): 448–461. https://doi.org/10.1016/j.engstruct.2013.11.006.

Van Nimmen, K., P. Van den Broeck, G. Lombaert, and F. Tubino. 2020. "Pedestrian-induced vibrations of footbridges: An extended spectral aproach." *J. Bridge Eng.* 25 (8): 04020058. https://doi.org/10.1061/(ASCE)BE.1943-5592.0001582.

Wan, K., S. Živanović, and A. Pavić. 2009. "Design spectra for single person loading scenario on footbridges." In *IMAC XXVII Conf. Exposition on Structural Dynamics*, Bethel, Conn: Society for Experimental Mechanics.

Wang, J., J. Chen, Y. Yokoyama, and J. Xiong. 2020. "Spectral model for crowd walking load." *J. Struct. Eng.* 146 (3): 04019220. https://doi.org/10.1061/(ASCE)ST.1943-541X.0002514.

Wei, X., J. Russell, S. Živanović, and J. T. Mottram. 2019. "Measured dynamic properties for FRP footbridges and their critical comparison against structures made of conventional construction materials." *Compos. Struct.* 223: 110956. https://doi.org/10.1016/j.compstruct.2019.110956.

Younis, A., O. Avci, M. Hussein, B. Davis, and P. Reynolds. 2017. "Dynamic forces induced by a single pedestrian: A literature review." *Appl. Mech. Rev.* 69 (2): 020802. https://doi.org/10.1115/1.4036327.

Zivanović, S., A. Pavic, and P. Reynolds. 2007. "Probability-based prediction of multi-mode vibration response to walking excitation." *Eng. Struct.* 29 (6): 942–954. https://doi.org/10.1016/j.engstruct.2006.07.004.